Plant Physiol. (1992) 100, 565–575
0032-0889/92/100/0565/11/$01.00/0

Received for publication March 17, 1992
Accepted June 10, 1992

Iron-Induced Changes in Light Harvesting and Photochemical Energy Conversion Processes in Eukaryotic Marine Algae[1]

Richard M. Greene*, Richard J. Geider, Zbigniew Kolber, and Paul G. Falkowski

Oceanographic and Atmospheric Sciences Division, Brookhaven National Laboratory, Upton, New York 11973 (R.M.G., Z.K., P.G.F.); and College of Marine Studies, University of Delaware, Lewes, Delaware 19958 (R.J.G.)

ABSTRACT

The role of iron in regulating light harvesting and photochemical energy conversion processes was examined in the marine unicellular chlorophyte *Dunaliella tertiolecta* and the marine diatom *Phaeodactylum tricornutum*. In both species, iron limitation led to a reduction in cellular chlorophyll concentrations, but an increase in the in vivo, chlorophyll-specific, optical absorption cross-sections. Moreover, the absorption cross-section of photosystem II, a measure of the photon target area of the traps, was higher in iron-limited cells and decreased rapidly following iron addition. Iron-limited cells exhibited reduced variable/maximum fluorescence ratios and a reduced fluorescence per unit absorption at all wavelengths between 400 and 575 nm. Following iron addition, variable/maximum fluorescence ratios increased rapidly, reaching 90% of the maximum within 18 to 25 h. Thus, although more light was absorbed per unit of chlorophyll, iron limitation reduced the transfer efficiency of excitation energy in photosystem II. The half-time for the oxidation of primary electron acceptor of photosystem II, calculated from the kinetics of decay of variable maximum fluorescence, increased 2-fold under iron limitation. Quantitative analysis of western blots revealed that cytochrome *f* and subunit IV (the plastoquinone-docking protein) of the cytochrome b_6/f complex were also significantly reduced by lack of iron; recovery from iron limitation was completely inhibited by either cycloheximide or chloramphenicol. The recovery of maximum photosynthetic energy conversion efficiency occurs in three stages: (a) a rapid (3–5 h) increase in electron transfer rates on the acceptor side of photosystem II correlated with de novo synthesis of the cytochrome b_6/f complex; (b) an increase (10–15 h) in the quantum efficiency correlated with an increase in D1 accumulation; and (c) a slow (>18 h) increase in chlorophyll levels accompanied by an increase in the efficiency of energy transfer from the light-harvesting chlorophyll proteins to the reaction centers.

Phytoplankton photosynthesis in the world's oceans accounts for approximately 40% of global carbon fixation, yet identification of the factors limiting primary productivity and phytoplankton biomass has been elusive. Low phytoplankton biomass in the surface waters of the central ocean basins (Fig. 1) has been attributed to limitation by inorganic nitrogen (12). Measurements of maximum quantum yields of photosynthesis (5) and fluorescence (15, 21) in both coastal and oceanic waters suggest that nutrients limit phytoplankton photosynthesis and growth. However, large regions of the subarctic Pacific, equatorial Pacific, and the Southern Ocean have excess inorganic nitrogen and phosphorus but low phytoplankton biomass (Fig. 1). In these high-nutrient, low-Chl regions, dissolved Fe concentrations are vanishingly low (<0.05 nM, [26]). In oceanic regions far removed from land or shallow benthic regeneration sites, the primary source of Fe is from atmospheric deposition; the lowest inputs of atmospheric Fe occur in the south central Pacific and Southern Ocean (9). Fe enrichment to natural phytoplankton samples from these waters stimulates net Chl synthesis and nitrate utilization, implying that Fe limits phytoplankton photosynthesis and growth in large regions of the world's oceans (26). However, the interpretation of Fe enrichment bottle experiments, and thus the Fe limitation hypothesis, is controversial (1), and supporting physiological evidence from natural phytoplankton communities is scant.

It is well documented that Fe is essential for Chl biosynthesis and inorganic nitrogen assimilation, and is an important redox catalyst in electron transport reactions in green plants and cyanobacteria (30). Consequently, Fe availability may be an important factor affecting thylakoid membrane structure and function and the basic processes involved in photochemical energy conversion. In the PSII complex, the efficiency of photochemical energy conversion depends on processes involved in light harvesting, excitation energy trapping and primary charge separation, stabilization of charge separation on secondary acceptors, and the repopulation of the primary electron donor leading to the oxidation of water. A common effect of Fe limitation is the reduction in pigment concentration, a concomitant decrease in the maximum Chl-specific rate of photosynthesis, and an increase in fluorescence per unit of Chl (16, 27, 30). Moreover, quantum yields of O_2 evolution and in vivo fluorescence (16, 27) are reduced under Fe limitation, in spite of an increase in light absorption per unit Chl, suggesting that Fe limitation alters the efficiency of excitation energy transfer from the antenna to the reaction centers in PSII.

Measurements of the in vivo fluorescence of Chl *a* provides rapid information on photochemical energy conversion processes and PSII integrity. The ratio of variable to maximum

[1] Supported by the U.S. Department of Energy under contract No. DE-AC02-76CH00016, the National Science Foundation grant No. OCE8915084 (to R.J.G.), National Aeronautics and Space Administration grant UPN 161-35-05-08 (to P.G.F.), and the Environmental Protection Agency grant No. DW89935239-01-0 (to P.G.F.).

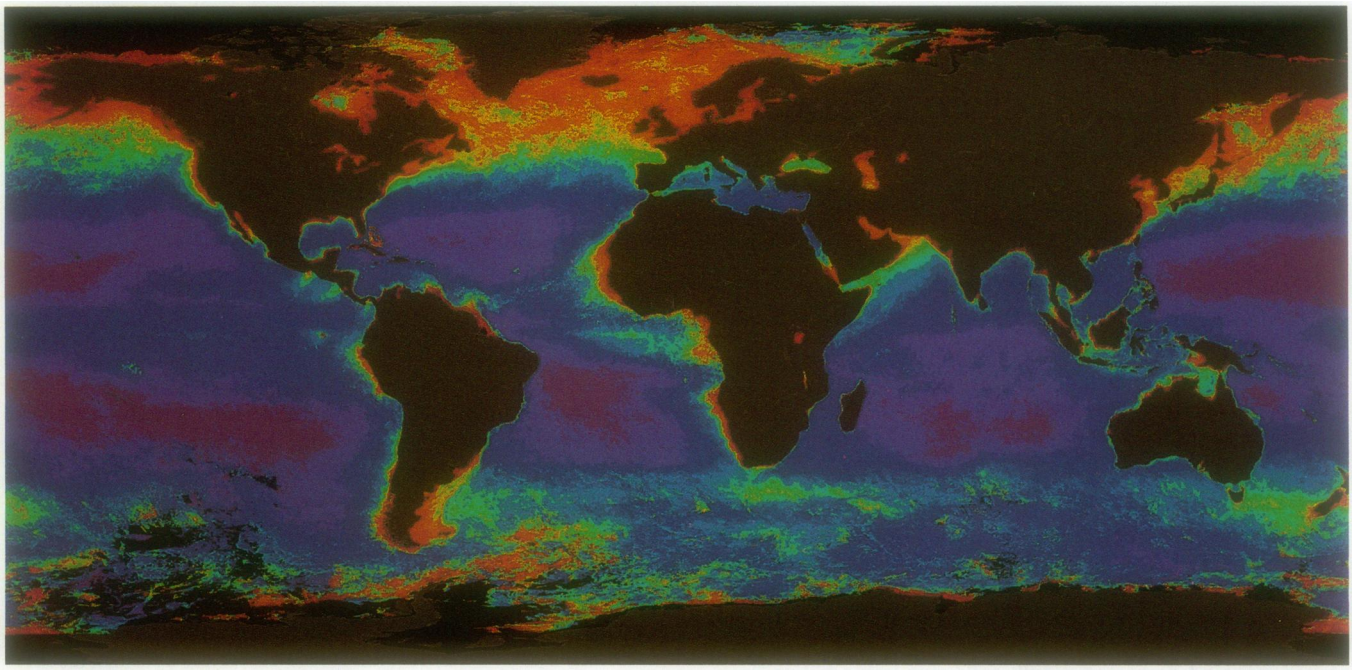

Figure 1. False-color satellite map of Chl distributions in the world's oceans averaged over an 8-year period from 1978 to 1986. Low Chl concentrations (<0.01 μg L^{-1}) are shown in purple, and high concentrations (>1.0 μg L^{-1}) are shown in red. Note the relatively low Chl concentrations in the subarctic Pacific, equatorial Pacific, and Southern Ocean. Unlike other open ocean regions, these areas have excess inorganic nitrogen and phosphorus, but exceedingly low dissolved Fe concentrations. Photograph courtesy of G. Feldman, Goddard Space Flight Center.

fluorescence (F_v/F_m, where $F_v = F_m - F_o$)[2] is a quantitative measure of the quantum efficiency of PSII photochemistry (20). Maximum quantum efficiency depends on the efficient transfer of excitation energy to the reaction centers and on fully functional and open reaction centers. Environmental factors that damage or alter the structure and function of the photosynthetic apparatus can lead to marked reductions in quantum efficiency. Although previous studies have shown that in vivo fluorescence characteristics and quantum efficiencies are altered under Fe limitation (16, 27), the specific mechanisms of the response are unknown.

Here we examine Fe-induced changes in the structure and function of the photosynthetic apparatus in the marine chlorophyte *Dunaliella tertiolecta* and the marine diatom *Phaeodactylum tricornutum* during the recovery from Fe limitation. Using pump-and-probe fluorescence techniques, as well as Fe-induced changes in light-absorption properties, we measured changes in the quantum efficiency and absorption cross-sections of PSII and the kinetics of Q_a^- oxidation. The theoretical basis of the pump-and-probe technique has been described (14, 22). The fluorescence-based changes were interpreted in relation to Fe-induced changes in the abundance of specific photosynthetic proteins, using immunological analyses, metabolic inhibitors, and ^{59}Fe radiolabeling studies. The results provide a mechanistic basis for understanding the role of Fe in light harvesting and photochemical energy conversion processes.

[2] Abbreviations: F_o, F_m, and F_v are initial, maximal, and variable fluorescence yields; ASW, artificial seawater; RCII, reaction center of PSII; PQ, plastoquinone; Q_a, primary electron acceptor of PSII; Q_b, secondary electron acceptor of PSII; $\Delta\phi_{sat}$, quantum yield.

MATERIALS AND METHODS

Culture Conditions

Stock cultures of *Dunaliella tertiolecta* (clone DUN) and *Phaeodactylum tricornutum* (clone Phaeo) were grown in 1-L polycarbonate flasks in an ASW medium enriched with f/2 nutrients (17). Fe was added separately as $FeCl_3$/EDTA to a final concentration of 25 nM Fe. Media and nutrients were filter sterilized to 0.2 μm using hollow fiber filters (MediaKap, Microgon, Inc., Laguna Hills, CA). All plasticware was washed with 10% HCl and rinsed with distilled H_2O. Cells were grown at 18°C under continuous light (250 μmol quanta m^{-2} s^{-1}), provided by banks of cool-white fluorescent tubes, with constant aeration and mixing. Fe-limited cells, growing at a specific growth rate of 0.1 d^{-1}, were obtained from early stationary-phase cultures. The recovery from Fe limitation was initiated by diluting 700 mL of stock culture (1.5×10^6 cells mL^{-1}) into 8 L of fresh media containing 250 nM Fe. Cells were enumerated with a hemocytometer. Following the transfer to high-Fe media, changes in cellular pigment concentration, absorption cross-sections, in vivo fluorescence characteristics, and abundance of photosynthetic proteins were monitored at several time points during the recovery from Fe limitation.

Pigment Concentration and in Vivo Absorption Spectra

Pigment concentrations were determined in 90% acetone extracts using the equations of Jeffrey and Humphrey (18) for Chl *a*, *b*, and *c*, and an extinction coefficient ($E_{1\%}$) of 2500 mM^{-1} at 480 nm for total carotenoids (6). In vivo absorption spectra were measured from 375 to 750 nm in unconcentrated cell suspensions using an Aminco DW2C spectrophotometer with ASW in the reference cell. To reduce light scattering, the samples were placed close (<1 cm) to the end window of the 2-inch photomultiplier. Both reference and measuring beams were diffused by a frosted quartz filter placed in front of the photomultiplier. In vivo absorption spectra normalized to Chl *a* (a^*_λ) were calculated at 12 wavelength intervals between 400 and 700 nm (11). The spectrally averaged, in vivo absorption cross-section, a^* (m^2 [mg Chl *a*]$^{-1}$), was calculated using the spectral distribution of both a quartz-halogen lamp (white light) and the xenon flash lamp (blue light) used for pump-and-probe fluorescence measurements (see below):

$$a^* = \frac{\Sigma\ (a^*_\lambda\ I_\lambda\ \Delta\lambda_i)}{\Sigma\ (I_\lambda\ \Delta\lambda)} \quad (1)$$

where $\Delta\lambda$ is the wavelength interval of the spectral band between 400 and 700 nm and I_λ is the irradiance in spectral band $\Delta\lambda_i$ (11). Converting a^* from m^2 (mg Chl *a*)$^{-1}$ to $Å^2$ (molecule Chl *a*)$^{-1}$ allows calculation of the apparent average optical absorption cross-section of a single Chl *a* molecule (σ_{Chl}). Spectral irradiance was measured with a Biospherical Instruments MER 1000 spectroradiometer equipped with a custom-made 0.75-inch diameter fiber-optic light guide.

Fluorescence Measurements

In vivo fluorescence measurements were made using a custom-built pump-and-probe fluorometer described by Kolber et al. (22). Flashes were provided by xenon flash lamps (EG&G 12B-1.5); broad band, blue-green light was isolated with a combination of Corning 4–76 and 4–96 filters. Actinic pump flashes had a 1.6-μs half-peak duration and a maximum intensity of approximately 10^{15} quanta cm^{-2}. The energy of the probe flash was attenuated to 0.5% of the actinic flash and had a half-peak duration of 0.7 μs. Fluorescence emission was detected by a Hamamatsu R2066 photomultiplier protected by an IR-absorbing glass filter, two 690-nm interference filters, and a 680-nm sharp cutoff filter. Fluorescence from the probe flash was measured before (designated F_o) and 80 μs after a pump flash of variable intensity (designated F). Cell suspensions were kept in darkness for a prolonged period (generally 30 min) prior to measuring F_o. F_m was measured following a pump flash of saturating intensity. The ratio of variable/maximum fluorescence (F_v/F_m, where $F_v = F_m - F_o$) was calculated at each time point during the recovery period.

Flash intensity saturation curves for the change in the quantum yield of fluorescence ($\Delta\phi = [F - F_o]/F_o$) were fit to a cumulative one-hit Poisson distribution (24, 25):

$$\Delta\phi = \Delta\phi_{sat}\ [1 - \exp(-\sigma_{PSII}\ E)] \quad (2)$$

where $\Delta\phi_{sat}$ is the change in maximum fluorescence yield ($[F_m - F_o]/F_o$), σ_{PSII} is the absorption cross-section of PSII ($Å^2$ quanta^{-1}), and E is the flash energy. The decay of $\Delta\phi_{sat}$ was measured by increasing the delay time between the saturating pump flash and the second probe flash from 80 μs to 500 ms. The kinetic parameters of the decay of $\Delta\phi_{sat}$ were obtained from a three-component exponential model (22) of the form:

$$\Delta\phi(t) = \alpha_1 \exp(-t/\tau_1) + \alpha_2 \exp(-t/\tau_2) + \alpha_3 \exp(-t/\tau_3) \quad (3)$$

where τ_n is the turnover time of component n, α_n is the relative amplitude associated with each τ_n, and t is the time delay.

Fluorescence induction curves were measured on Fe-limited and Fe-replete cultures in the absence and presence of 10 μM DCMU. The samples were dark adapted for 30 min and placed in a 1-cm pathlength cuvette located close to the end window of a 2-inch photomultiplier. Actinic illumination (3×10^{16} quanta cm^{-2} s^{-1}) from a xenon arc lamp (Oriel Corp., Stratford, CT) was directed to the front of the cuvette by a fiber-optic light guide and controlled by an electronic shutter. Broad-band blue light was isolated with a Corning 4–96 filter and was passed through an IR and UV filter. The photomultiplier was protected by a 700-nm interference filter and a Corning 2–64 band pass filter. The kinetics of the fluorescence rise curves were recorded on a digital storage oscilloscope, and the digital data were transferred to a computer for further analysis. The ratio, in electron equivalents, of PQ/Q_a was calculated from the area over the induction curves.

Room-temperature fluorescence excitation spectra were measured on Fe-limited and Fe-replete *P. tricornutum* cell suspensions with an SLM 4800S spectrofluorometer. Excitation spectra were normalized to the in vivo absorption spectra between 400 and 600 nm.

Protein Analysis

Cells were harvested at different time points following the addition of Fe to Fe-limited cultures. Samples were concentrated by centrifugation and washed in 10 mM Tris buffer containing 0.4 M NaCl and 10 mM EDTA. Cells were disrupted on ice in 100 μL of 8% SDS, 0.2 M Na_2CO_3, and 200 μM PMSF by three 30-s sonication cycles using a Kontes microprobe sonicator on maximum power. Samples were centrifuged at 14,000 rpm in an Eppendorf microcentrifuge for 5 min to pellet debris. Subsamples from the supernatant were removed for analysis of Chl and protein content. Chl was determined on a 5-μL subsample dissolved in 1 mL of 90% acetone using the equations of Jeffrey and Humphrey (18). Total protein was determined using the Pierce (Rockford, IL) bicinchoninic acid assay, following the manufacturer's guidelines. The remainder of the sample was diluted with a equal volume of 0.2 M DTT and 2 volumes of 4% SDS, 15% glycerol, and 0.05% bromthymol blue. The sample was then quick frozen in liquid N_2 and stored at −80°C until further analysis.

Proteins were separated by SDS-PAGE using a Bio-Rad (Rockville Center, NY) mini-gel system, with a 7% stacking and 15% resolving gel. Samples containing 25 μg of protein

were loaded into each lane and run at constant voltage (125 V) for 1.5 to 2 h at room temperature. Following electrophoresis, gels were either stained with Coomassie blue or transferred to nitrocellulose. Photosynthetic proteins were detected by immunological analysis using polyclonal antibodies raised against the proteins of interest. Fe-induced changes in the relative abundance of five specific proteins were examined. D1, the 32-kD reaction center II protein, Cyt *f* and subunit IV of the Cyt b_6/f complex, and the large subunit of Rubisco are encoded in the chloroplast genome, whereas the light-harvesting Chl proteins are nuclear encoded (13). With the exception of Rubisco, all the proteins are integral components of the thylakoid membranes. Protein abundance was quantified by laser densitometry.

Radiolabeling and Translational Inhibitors

The effect of translational inhibitors on in vivo fluorescence characteristics and on the incorporation of radiolabeled ^{59}Fe into proteins was examined during the recovery from Fe limitation. Cells were grown to stationary phase in low-Fe ASW as described above. Two hundred-milliliter aliquots with a cell density of 1.6×10^6 mL^{-1} were dispensed into 250-mL bottles. Cycloheximide, an inhibitor of nuclear-encoded protein synthesis, was added to three bottles to a final concentration of 0.1, 1.0, and 10.0 μg mL^{-1}. Chloramphenicol, an inhibitor of chloroplast-encoded protein synthesis, was added to another three bottles to a final concentration of 5, 50, and 500 μg mL^{-1}. After a 1-h incubation, $FeCl_3$/EDTA was added to a final concentration of 70 nM. Control bottles without inhibitors contained either 70 nM Fe (designated +Fe control) or no added Fe (designated −Fe control). After a 15-h recovery period, the samples were collected for cell counts, pigment analyses, and in vivo fluorescence characteristics as described above. In a duplicate experiment, radiolabeled $^{59}FeCl_3$/EDTA (specific activity = 61 mCi mg^{-1}, 70 nM final concentration) was added to Fe-limited cultures in the presence and absence of inhibitors. After a 15-h recovery period, the samples were collected for SDS-PAGE and transferred to nitrocellulose. The effect of inhibitors on the incorporation of radiolabel was analyzed on autoradiograms developed at −80°C for 15 d using laser densitometry.

RESULTS

Cell Growth, Pigmentation, and in Vivo Absorption Cross-Sections during Fe-Induced Recovery

The addition of $FeCl_3$ to Fe-limited cells resulted in the initiation of Chl synthesis and cell division after a lag period of 9 to 18 h, respectively, in *D. tertiolecta* (Fig. 2, A and B), and of 15 to 24 h in *P. tricornutum* (Fig. 2, E and F). Following the initial lag period, total Chl concentrations increased 2-fold in *D. tertiolecta* and 5-fold in *P. tricornutum* during the remainder of the recovery period. At about 60 h into the recovery period, *P. tricornutum* and *D. tertiolecta* had achieved growth rates equivalent to about 30 and 75%, respectively, of their maximum rates (1.6 d^{-1}) under our culture conditions. Total carotenoid:Chl *a* ratios decreased following an initial lag period of 9 to 13 h (Fig. 2, C and G), reflecting the increase in cellular Chl *a* concentration. Chl *b*:*a* and *c*:*a* ratios in

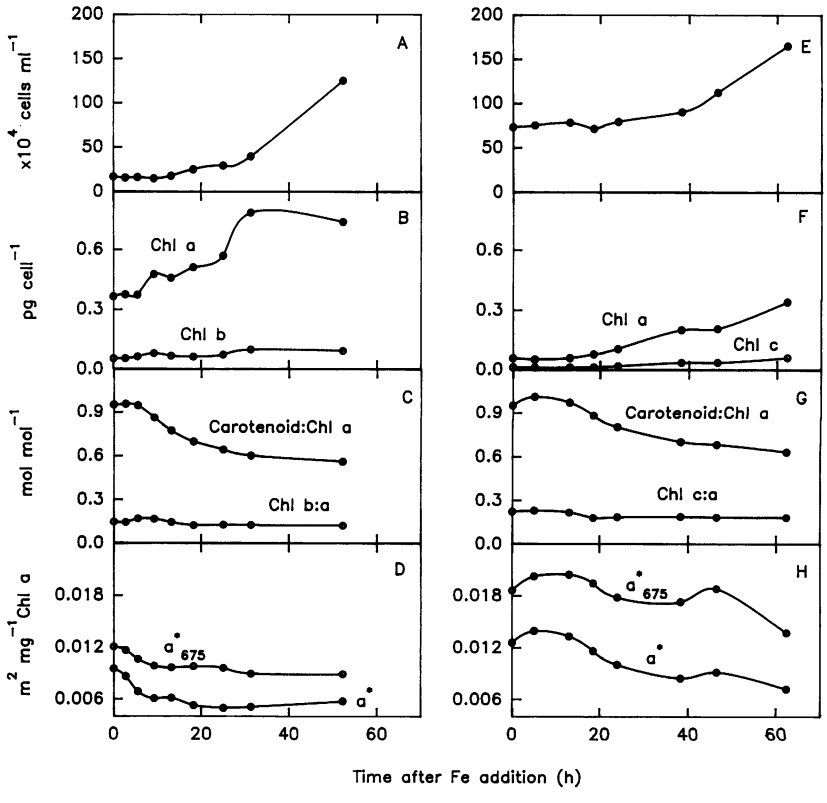

Figure 2. Time course for the recovery of cell numbers (A and E), pigment concentration (B and F), pigment ratios (C and G), and in vivo absorption cross-sections (D and H) in *D. tertiolecta* (left panels) and *P. tricornutum* (right panels) following the addition of Fe to Fe-limited cells.

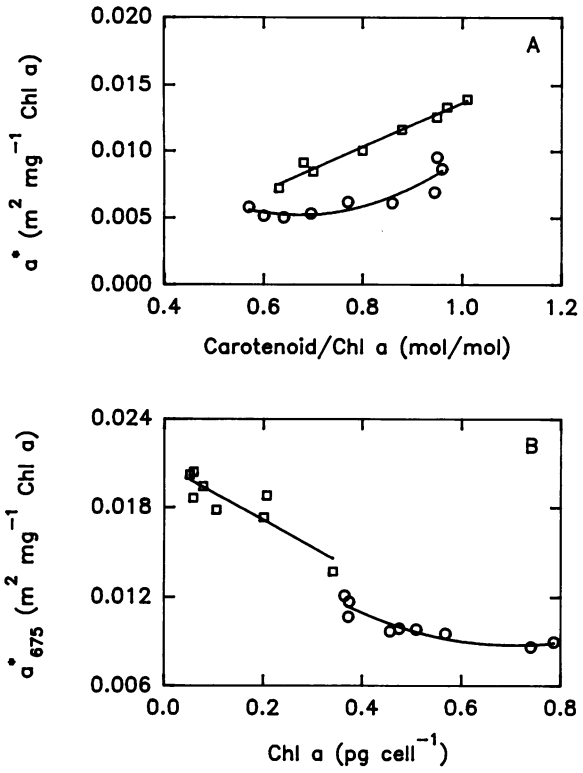

Figure 3. Relationship between (A) in vivo absorption cross-section (a*) and carotenoid:Chl *a* ratios, and (B) in vivo absorption at 675 nm and intracellular Chl *a* concentration, in *D. tertiolecta* (O) and *P. tricornutum* (□) during the recovery from Fe limitation. Solid lines represent the least-squares regression.

D. tertiolecta and *P. tricornutum*, respectively, decreased about 20% during the recovery period.

The spectrally averaged, in vivo absorption cross-section (a^*) was high in Fe-limited cells, and decreased 90 to 95% following Fe addition (Fig. 2, D and H). Variations in a^* can be attributed to changes in cellular pigmentation, changes in the extent of thylakoid stacking or transparency, or to changes in chloroplast size (2). The latter characteristics contribute to what is referred to as the "package effect" and reflect the optical properties of a heterogeneous suspension of particles. During the recovery from Fe limitation, variations in a^* were highly correlated with carotenoid:Chl *a* ratios (Fig. 3A; r^2 = 0.99 and 0.90 for *P. tricornutum* and *D. tertiolecta*, respectively). At 675 nm, there is no effect of carotenoids on a^*, and changes in the cross-section at this wavelength only reflect changes in the package effect (2). a^*_{675} declined 35% in *D. tertiolecta* and 46% in *P. tricornutum* during the recovery period (Fig. 2, D and H), and was highly correlated with intracellular Chl *a* concentration (Fig. 3B; r^2 = 0.88 and 0.93, respectively). Thus, about 39% ($\Delta a^*_{675}/\Delta a^*$ = 35/90) of the change in the in vivo absorption cross-section of *D. tertiolecta* can be ascribed to changes in the package effect, and the remaining 61% to changes in pigmentation associated with the Fe recovery process. In *P. tricornutum*, changes in the package effect accounted for 49%, and changes in intracellular pigmentation accounted for 51% of the change in a^*.

In Vivo Fluorescence Characteristics during Fe-Induced Recovery

F_v/F_m increased rapidly following the addition of Fe to Fe-limited cells, reaching about 90% of its maximum value within 18 h in *D. tertiolecta* (Fig. 4A) and within 25 h in *P. tricornutum* (Fig. 4D). When normalized to Chl *a* concentration, F_m^{Chl} initially increased and then decreased during the

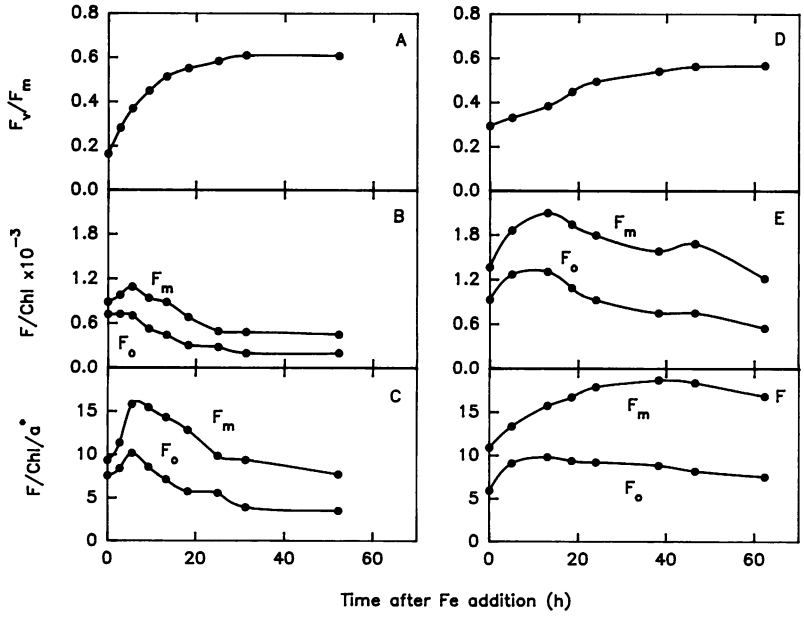

Figure 4. Time course for the recovery of F_v/F_m (A and D), fluorescence normalized to Chl *a* (B and E), and fluorescence yield (fluorescence per unit of Chl *a* normalized to a^*) (C and F) in *D. tertiolecta* (left panels) and *P. tricornutum* (right panels) following the addition of Fe to Fe-limited cells.

remainder of the recovery period (Fig. 4, B and E); F_o^{Chl} in *P. tricornutum* exhibited a similar pattern (Fig. 4E). In *D. tertiolecta*, however, F_o^{Chl} was constant during the initial stages, and then declined during the remainder of the recovery (Fig. 4B). To account for changes in the efficiency of light absorption during the recovery period, F_m^{Chl} and F_o^{Chl} were normalized to a^*. In *P. tricornutum*, fluorescence yield (F^{Chl}/a^*) at F_o initially increased and then remained constant, whereas fluorescence yield at F_m continued to increase throughout much of the recovery period (Fig. 4F). The decrease in fluorescence yield (fluorescence/absorption) at all wavelengths between 400 and 575 nm in Fe-limited *P. tricornutum* (Fig. 5) indicated that excitation energy transfer from both Chl and carotenoids was reduced under Fe limitation, consistent with the differences in F^{Chl}/a^* shown in Figure 4. The changes in in vivo fluorescence and absorption characteristics indicated a reduction in the transfer efficiency of excitation energy from the antenna to the reaction centers in Fe-limited *P. tricornutum*. In *D. tertiolecta*, fluorescence yield (F^{Chl}/a^*) at both F_m and F_o declined following the initial increase (Fig. 4C).

The absorption cross-section of PSII (σ_{PSII}), calculated from flash-intensity saturation curves of fluorescence yield (Eq. 2), decreased following Fe addition from 187 to 75 $Å^2$ quanta^{-1} in *D. tertiolecta* and from 280 to 160 $Å^2$ quanta^{-1} in *P. tricornutum* (Fig. 6A). Recovery from Fe limitation shifts the flash-intensity saturation curves toward higher flash intensities (i.e. more light is required to saturate the fluorescence yield curve; Fig. 6B). Previous results demonstrated that Fe limitation in *P. tricornutum* increased σ_{PSII} and decreased I_k, the irradiance at which O_2 evolution becomes light saturated (16).

Recovery from Fe limitation resulted in flash-intensity saturation curves that increased faster than the exponential behavior described by the Poisson function (Fig. 6B). This behavior has been suggested to result from the migration of excitation energy from closed to open reaction centers (29). Using the equations of Paillotin (29), the probability, P, of energy transfer between reaction centers was calculated for

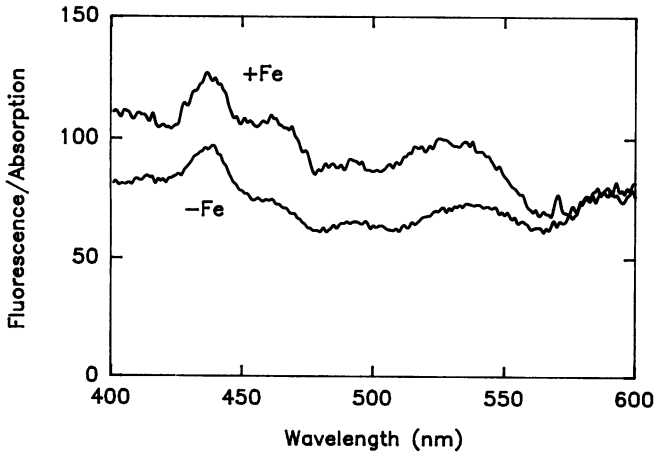

Figure 5. Spectra of fluorescence normalized to light absorption between 400 and 600 nm in Fe-limited (−Fe) and Fe-replete (+Fe) *P. tricornutum*.

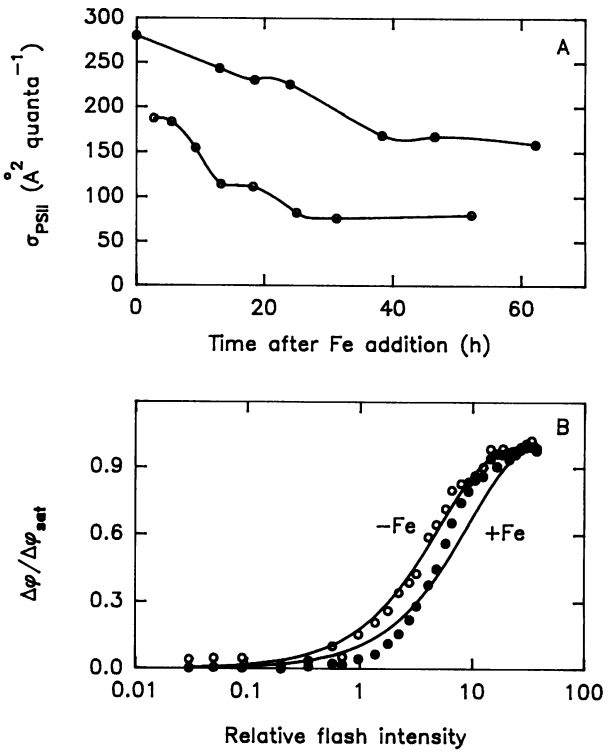

Figure 6. A, Changes in the absorption cross-section of PSII (σ_{PSII}) during the recovery from Fe limitation in *D. tertiolecta* (○) and *P. tricornutum* (●). B, Representative flash-intensity saturation curves for changes in fluorescence yield, normalized to the maximum yield, in Fe-limited (−Fe) and Fe-replete (+Fe) *D. tertiolecta*.

both species during the recovery period. These calculations indicated that P increased from 0.3 to 0.9 during the recovery from Fe limitation.

The recovery of F_v/F_m and σ_{PSII} following Fe addition was sensitive to the addition of cycloheximide and chloramphenicol. In general, low inhibitor concentrations partially prevented the recovery of F_v/F_m and σ_{PSII} (Table I). High inhibitor concentrations completely blocked the recovery process; at these concentrations, F_v/F_m was lower than the Fe-limited controls. In control cultures without inhibitors, the addition of Fe increased F_v/F_m about 2-fold during the 15-h recovery period (Table I).

The kinetics of the decay of $\Delta\phi_{sat}$ following a single saturating flash varied between Fe-replete and Fe-limited cells. When normalized to the maximum yield, Fe-limited cells exhibited a much slower decay response at the short delay times (Fig. 7A). The fast component of the decay kinetics (τ_1, calculated from Eq. 3) averaged about 400 μs in Fe-limited cells. τ_1 corresponds to the half-time for the transfer of a single electron from Q_a^- to Q_b (22). τ_1 declined rapidly during the recovery from Fe limitation, approaching the steady-state, Fe-replete value (160–200 μs) with a first-order decay response (Fig. 7B); the half-time for the recovery of τ_1 was calculated at 1.6 and 2.5 h for *P. tricornutum* and *D. tertiolecta*, respectively.

Fe limitation resulted in modifications in the shape of the fluorescence induction curve. The rise time from F_o to F_m (i.e.

Table I. *Effect of Translational Inhibitors on F_v/F_m and the Absorption Cross-Section of PSII (σ_{PSII}, $Å^2$ quanta^{-1}) during Recovery from Fe Limitation in D. tertiolecta and P. tricornutum*

Fe-limited cultures were incubated with various inhibitor concentrations (μg/mL) for 1 h prior to the addition of Fe/EDTA to a final concentration of 70 nM Fe. In vivo fluorescence characteristics were determined on dark-adapted cells using a pump-and-probe fluorometer after a 15-h incubation.

Treatment	*D. tertiolecta*		*P. tricornutum*	
	F_v/F_m	σ_{PSII}	F_v/F_m	σ_{PSII}
Controls				
−Fe	0.26	150	0.30	178
+Fe	0.40	116	0.48	83
Cycloheximide				
0.1	0.37	130	0.32	280
1.0	0.31	133	0.23	355
10.0	0.23	128	0.15	360
Chloramphenicol				
5	0.38	101	0.42	218
50	0.41	110	0.37	265
500	0.18	146	0.06	821

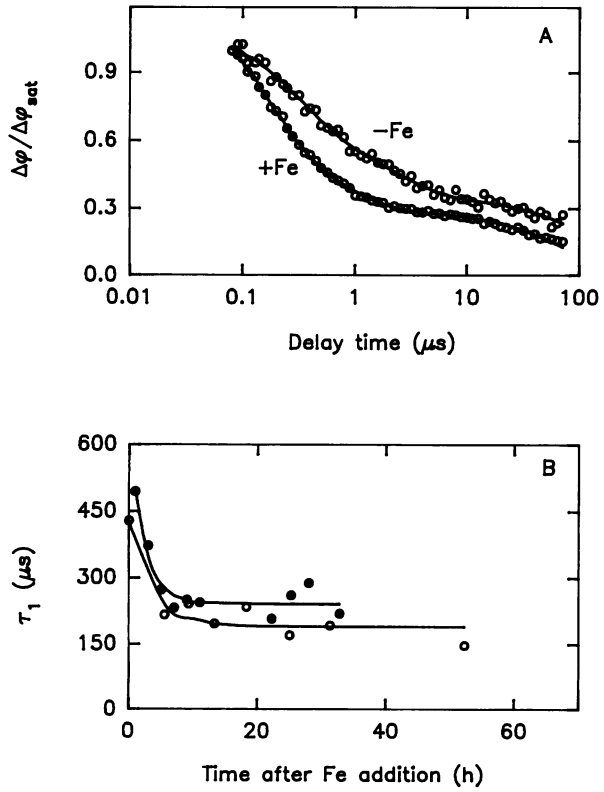

Figure 7. A, Representative curves of the decay kinetics of $\Delta\phi_{sat}$ in Fe-limited (−Fe) and Fe-replete (+Fe) *D. tertiolecta*. B, Time course of changes in the fast turnover time (τ_1) of electron transfer reactions on the acceptor side of PSII during the recovery from Fe limitation in *D. tertiolecta* (○) and *P. tricornutum* (●).

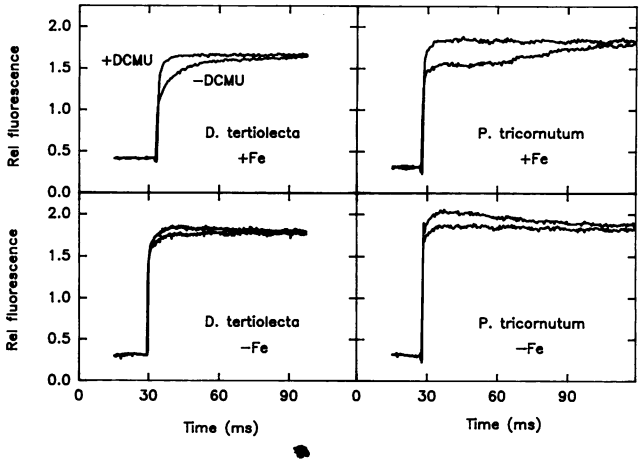

Figure 8. Fluorescence induction response in Fe-limited (−Fe) and Fe-replete (+Fe) cells of *D. tertiolecta* and *P. tricornutum*. The top and bottom traces in each panel represent the induction response in the presence and absence, respectively, of 10 μM DCMU.

the variable fluorescence component) was significantly shorter in Fe-limited cells relative to Fe-replete cells (Fig. 8). The area over the induction curves in the presence and absence of DCMU can be used to calculate the ratio PQ/Q_a in electron equivalents; in the absence of DCMU, the area is inversely proportional to the number of PSII turnovers required to reduce the PQ pool, whereas upon addition of DCMU and assuming no "leakage" of electrons from Q_a, the area reflects the number of electron equivalents required to reduce the Q_a pool. In Fe-replete *P. tricornutum* and *D. tertiolecta*, the PQ/Q_a ratio averaged 14.3 (SD = 7.3) and 5.2 (SD = 3.2), respectively. In Fe-limited cells, the ratio was reduced to 0.7 (SD = 0.1) and 1.5 (SD = 0.4), respectively. Thus, the number of reducing equivalents in the PQ pool, relative to PSII reaction centers, was 5 to 15 times smaller in Fe-limited cells than in Fe-replete cells.

Changes in Protein Abundance during Fe-Induced Recovery

The addition of Fe to Fe-limited cells increased the relative abundance of photosynthetic proteins. The most rapid changes were observed in Cyt *f* abundance, which increased exponentially and reached a maximum at 14 h after Fe addition (Figs. 9 and 10); the relative abundance of Cyt *f* was 15 times lower in Fe-limited cells than in Fe-replete cells. The PSII reaction center protein (D1) increased 5-fold following Fe addition. In contrast to Cyt *f*, however, D1 exhibited a slower initial recovery (up to 11 h) followed by a more rapid linear increase between 11 and 18 h (Fig. 10). Subunit IV, the PQ-docking protein (10) in the Cyt b_6/f complex, increased 40-fold between 11 and 18 h following Fe addition; during the initial stages of the recovery period, subunit IV was not detectable by immunostaining (Figs. 9 and 10). The antibodies for Cyt *f* and subunit IV did not cross-react in *P. tricornutum*. Other photosynthetic proteins exhibited much smaller changes in response to Fe addition. There was a 2-fold increase in the large subunit of Rubisco, and a 1.5-fold increase in light harvesting Chl proteins (Figs. 9 and 10).

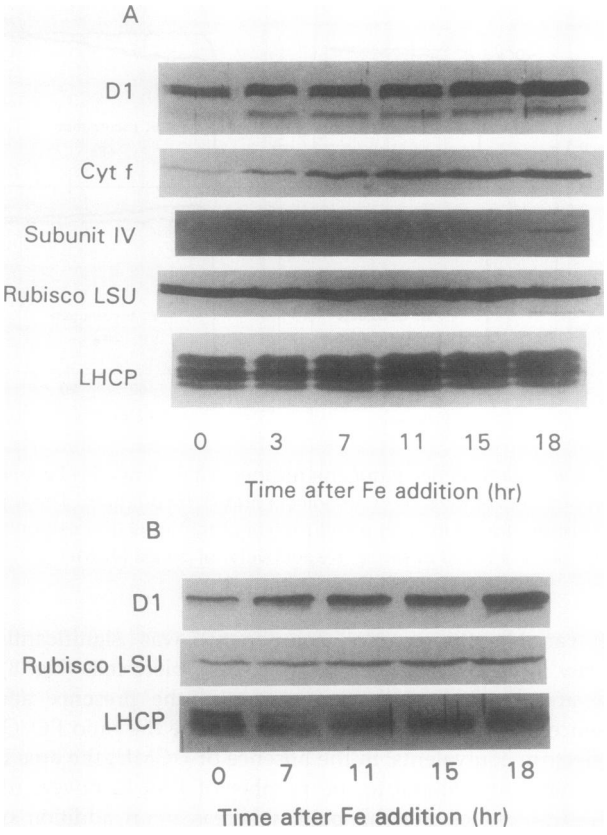

Figure 9. Western blots showing the changes in protein abundance in *D. tertiolecta (A),* and in *P. tricornutum* (B) during the recovery from Fe limitation. Total cell proteins were separated by SDS-PAGE and transferred to nitrocellulose. Each lane was loaded with 25 μg of protein. Immunoassays were conducted with polyclonal antibodies raised against the specific proteins of interest.

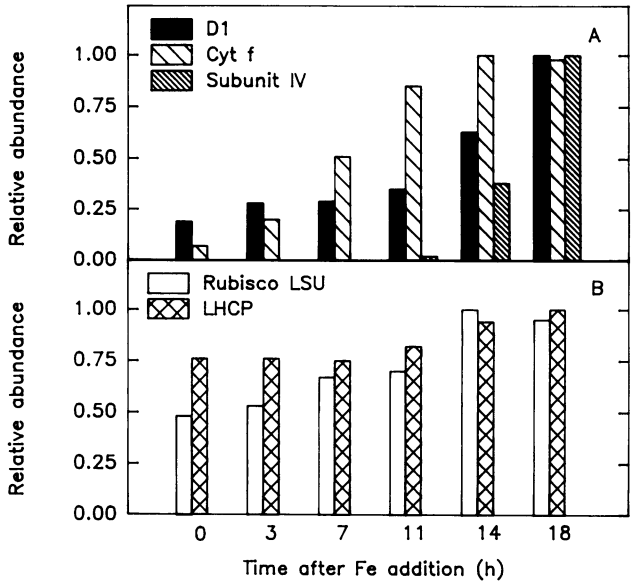

Figure 10. A and B, Quantitative changes in protein abundance, relative to the maximum abundance, during the recovery from Fe limitation in *D. tertiolecta*. Protein abundance (absorbance units × mm^2) was derived from laser densitometry of western blots shown in Figure 9A.

^{59}Fe Radiolabeling during Fe-Induced Recovery

In vivo labeling with ^{59}Fe during a 15-h recovery resulted in the incorporation of radiolabel into proteins with apparent molecular masses of 35, 20, and 15 kD. Based on immunological studies, these proteins were identified as Cyt *f*, the Rieske Fe-S protein, and Cyt b_{559}, respectively. Of the total amount of radiolabel detected in *D. tertiolecta*, 50% was present in Cyt *f*, 10% in the Rieske Fe-S protein, and 40% in the Cyt b_{559}. In *P. tricornutum*, 25% of the radiolabel was found in Cyt *f*, 31% in the Rieske Fe-S protein, and 44% in Cyt b_{559}. The addition of cycloheximide resulted in a large reduction in ^{59}Fe incorporation in Cyt *f* and Cyt b_{559} relative to controls without inhibitors (Table II); this effect was probably due to the inhibition of heme synthesis, which is directed by nuclear-encoded proteins. Low chloramphenicol concentrations had little effect on radiolabeling of the Cyt *f*, whereas Cyt b_{559} labeling was reduced to about 30 to 40% of controls; at high chloramphenicol concentrations, labeling of Cyt *f* was severely reduced.

DISCUSSION

Fe-Induced Changes in Quantum Efficiency and Fluorescence Quenching

Fe-induced changes in light absorption and in vivo fluorescence parameters can be described in relation to those processes that lower or quench the fluorescence yield below its maximum. Under conditions where all PSII traps are open:

$$F_o/A = k_f/(k_f + k_n + k_p{}^*f + k_s) \quad (4)$$

where A is the absorbed photon flux (a^*_{Chl}), k_f, k_n, and k_s are the rate constants for fluorescence, nonphotochemical quenching, and spillover, respectively, k_p is the rate constant for photochemistry by RCII, and f is the proportion of functional RCII ($0 \leq f \leq 1$). When all PSII traps are closed (i.e. when Q_a is fully reduced), k_p goes to zero and

Table II. *Quantitation of in Vivo Protein Labeling of ^{59}Fe in D. tertiolecta and P. tricornutum in the Absence (Designated "+Fe Control") and Presence of Translational Inhibitors*

Proteins were separated by SDS-PAGE, transferred to nitrocellulose, and developed on autoradiograms at −80°C for 15 d. Values for +Fe controls are the percentage of total label detected by densitometry; values for the various inhibitor concentrations (μg/mL) are presented as the percentage of label detected for each protein relative to +Fe controls.

	D. tertiolecta			*P. tricornutum*		
	Cyt *f*	Fe-S	Cyt b_{559}	Cyt *f*	Fe-S	Cyt b_{559}
			%			
+Fe control	50	10	40	25	31	44
Cycloheximide						
0.1	33	75	34	36	36	19
1.0	21	83	25	18	14	9
10.0	19	66	17	0	0	0
Chloramphenicol						
5	88	83	30	53	44	61
50	81	79	42	53	42	63
500	16	86	31	0	0	0

$$F_m/A = k_f/(k_f + k_n + k_s). \quad (5)$$

The quantum efficiency of PSII photochemistry is equal to the rate constant of primary photochemistry (k_p) divided by the sum of rate constants for all energy dissipation reactions (20, 23), and is equivalent to F_v/F_m (by rearrangement of Eqs. 4 and 5):

$$F_v/F_m = k_p{*}f/(k_f + k_n + k_p{*}f + k_s). \quad (6)$$

Because k_f and k_s are generally a small fraction (<5 to <10%) of the absorbed photon flux (23), any change in F_o/A and F_m/A must reflect changes in $k_p{*}f$ or k_n. If the rate constants do not vary, then changes in fluorescence emission must be due to changes in light absorption properties. It is important to note that factors that alter $k_p{*}f$ can only influence fluorescence emission from open traps, whereas changes in k_n affect fluorescence emission from both open and closed traps.

Our results suggest that in Fe-limited cells, photochemical quenching ($k_p{*}f$) was low. Photochemical quenching occurs in the reaction center and depends on the presence of oxidized Q_a and f, the proportion of functional RCIIs. As shown previously (16), the number of functional RCIIs determined from O_2 flash yields was low in Fe-limited *P. tricornutum*. The present study revealed that k_p was also low, as evidenced by the slow reoxidation kinetics of Q_a^-. In addition to a reduction in photochemical quenching, Fe limitation appeared to increase nonphotochemical quenching in *D. tertiolecta* and *P. tricornutum*. Nonphotochemical quenching (k_n) may occur in the antenna by xanthophyll cycle-related activities, or in the reaction center by "photoinhibitory"-like quenching (23). Fe-limited cells exhibited characteristics similar to photoinhibited cells, namely a reduction in F_o/A, F_m/A, and ϕ_m, the loss of D1, and a reduction in Chl-specific light-saturated photosynthesis (16). Although the molecular and biophysical mechanisms of photoinhibitory quenching are still unclear (23), it has been suggested that a fraction of RCIIs may be converted from photochemically functional to thermally quenching RCIIs (4). Our results suggest that formation of nonphotochemical quenching RCIIs may have been promoted by sluggish Q_a^- reoxidation rates (see below), allowing for an increased probability of thermal deexcitation.

Fe-Induced Changes on the Acceptor Side of PSII and the Cyt b_6/f Complex

The initial increase in F_v/F_m was correlated with a rapid decrease in the turnover time (τ_1) for electron transfer reactions on the acceptor side of PSII. A 2-fold change in τ_1 has been reported in studies comparing the decay kinetics of fluorescence yield in Fe-depleted and Fe-replete bacterial reaction centers (7, 19). A reduction in τ_1 should increase the lifetime of Q_a^-, resulting in reaction centers that appear closed to further excitations. This would create a "traffic jam" of excitons in the reaction center, leading to increased nonphotochemical quenching in RCII. Two phenomena could account for the Fe-induced changes in turnover times on the acceptor side of PSII. The first relates to the electron transfer kinetics of the two-electron quinone gate, and the second relates to the presence of a nonheme Fe^{2+} ion associated with Q_a and Q_b.

On the acceptor side of PSII, two photochemical events are required for the complete reduction of PQ. In this two-electron gate, the first electron is transferred from Q_a^- to Q_b in the 160- to 200-μs time range, whereas the second transfer to Q_b^- occurs in the 400- to 500-μs time range (7, 8, 23). Under our experimental conditions, in which the decay of $\Delta\phi_{sat}$ was measured following a single saturating pump flash, we assumed that τ_1 represented the transfer from Q_a^- to Q_b. If, however, Fe limitation altered the redox state or structural organization of electron acceptors between PSII and PSI, then the decay kinetics may have reflected electron transfer from Q_a^- to Q_b^-. We tested this hypothesis by measuring the decay kinetics of Fe-limited and Fe-replete cells following one or two saturating pump flashes. In Fe-replete cells, τ_1 increased 2-fold following a two-pump sequence (data not shown), consistent with previous studies (7, 8). In Fe-limited cells, τ_1 also increased 2-fold following two pump flashes. These results suggest that Fe limitation impeded both the first and second electron transfer steps, but does not change the redox state of the primary acceptor.

The alternative hypothesis for the Fe-induced changes in τ_1 relates to the presence of the nonheme Fe^{2+} closely associated with Q_a and Q_b (8). Although the exact function of this Fe^{2+} is not fully understood, it is thought to accept electrons directly from Q_a^-; however, under normal physiological conditions it does not undergo redox reactions (8). It is assumed that the Fe^{2+} ion plays an important role in electron transfer reactions in PSII, yet substitution by a number of divalent metals in bacterial reaction centers does not alter electron transfer kinetics (7).

The reoxidation of the plastoquinol depends on the functional integrity of the Cyt b_6/f complex. The relative abundance of proteins in the Cyt b_6/f complex changed rapidly following the addition of Fe to Fe-limited cells. This complex couples electron transport between PSII and PSI to proton translocation across the thylakoid membrane. During the recovery period, Cyt f accumulated faster than D1 and correlated with the initial recovery of F_v/F_m. Radiolabeling studies indicated that much of the ^{59}Fe was incorporated into Cyt f, and to a lesser extent in the Rieske Fe-S protein. However, not all proteins in the Cyt b_6/f complex accumulated at the same rate. Subunit IV, the PQ-docking protein (10), exhibited a lag of several hours, and then increased rapidly. Studies on higher plants indicate that the individual components of this complex biochemically turn over at different rates, and that all the components must be present for the stable assembly of a functional complex (3). Our results suggest that inhibition of the synthesis or assembly of the components into a functional complex, resulting from a lack of Fe, leads to an overreduction of the PQ pool and impedes the efficient transfer of electrons from the PSII to PSI.

Fe-Induced Changes in the RCII Core Complex

The latter phase of the recovery of F_v/F_m, and increase in $k_p{*}f$, was correlated with synthesis and repair of the RCII core complex, as evidenced by the increase in D1 abundance and ^{59}Fe incorporation into Cyt b_{559}. Chloramphenicol blocked this recovery process, suggesting that de novo protein synthesis is required. The accumulation of D1, and probably D2 as well, during recovery from Fe limitation may be related to conditions favoring the assembly of protein into the mem-

brane complex, because Fe does not appear to be directly involved in the regulation of D1 synthesis. D1 turns over rapidly under nutrient-replete conditions, several times faster than the growth rate, and about 50 to 60 times faster than the light-harvesting Chl proteins (28). We propose that D1 is synthesized under Fe-limited conditions but not integrated into the membrane complex. Furthermore, the ^{59}Fe-labeling results suggest that Cyt b_{559} synthesis was markedly reduced by Fe limitation. Cyt b_{559} is required to assemble functional PSII reaction centers. Thus, integration of D1 into the PSII core complex may be limited by the availability of Cyt b_{559} under Fe-limiting conditions.

Fe-induced synthesis and accumulation of D1 and Cyt b_{559}, and the increase in quantum efficiency, provides strong evidence for an Fe-induced increase in functional and open reaction centers. Under these conditions, more electrons per unit of Chl can be produced by a saturating flash. However, the stability of charge separation depends on the rapid transfer of electrons from phaeophytin to Q_a. When the transfer process is impeded by the reduction of Q_a from a previous excitation or by slow reoxidation kinetics (discussed above), the trap remains closed and the probability that excitation energy will be reemitted as fluorescence increases. Thus, Fe-induced changes in the redox state or structural organization of electron acceptors between PSII and PSI may have a significant effect on energy trapping and charge separation in RCII.

Optical and Functional Absorption Cross-Sections

The in vivo optical absorption cross section (a^*) is related to the average size of all antenna pigments serving both PSII and PSI reaction centers. The reduction in a^* during the recovery from Fe limitation reflected increasing intracellular Chl concentrations, and a concomitant increase in self-shading within the thylakoid membranes. As the density of Chl molecules in the membrane increased, the apparent absorption cross-section of Chl molecules (σ_{Chl}) decreased; this effect accounted for more than half of the change in a^* between Fe-limited and Fe-replete cells. Changes in thylakoid stacking or "transparency" (i.e. the density of pigment molecules per unit area of thylakoid membrane) probably also contributed to changes in the optical absorption cross-section during the recovery period. Berner et al. (2) demonstrated that in the single cup-shaped chloroplast of *D. tertiolecta*, the number of thylakoids per stack increased as a^*_{675} decreased. Thus, the probability of a photon being absorbed is higher in Fe-replete cells, due to an increased number of absorbing molecules and an increased number of thylakoids per stack, yet the effective light absorption per unit of Chl is reduced because the thylakoids become optically opaque.

The functional absorption cross-section of PSII (σ_{PSII}) reflects only those absorbing molecules that transfer excitation energy to the PSII reaction centers, and is a measure of the photon target area presented by PSII traps (24). Fe-induced changes in σ_{PSII} may be due to changes in several parameters, including σ_{Chl}, the number of antenna molecules serving a RCII, the number of functional RCIIs, or the quantum efficiency of photosynthesis (ϕ_m, see Eq. 7). In addition to changes in σ_{Chl} (described above), results of the present study indicated that the reduction in σ_{PSII} during the Fe-induced recovery period was correlated with a decrease in the ratio of antenna complexes relative to reaction center core complexes. Although Fe addition led to an increase in pigment per cell, there was less light-harvesting Chl proteins relative to D1. These effects are not unique to Fe limitation. N limitation in a variety of phytoplankton species reduced the abundance of D1, as well as CP 43 and CP 47 in the proximal antenna, relative to light-harvesting Chl proteins, and led to an increase in σ_{PSII} (13, 22).

The migration of excitation energy from closed to open RCIIs effectively increases σ_{PSII}. We tested the hypothesis that the probability of energy transfer was higher in Fe-replete cells due to a higher spatial density of reaction centers on the thylakoid membranes (i.e. each reaction center has a nearer "neighbor" in highly pigmented, Fe-replete cells). We blocked 50% of PSII reaction centers with 10^{-8} M DCMU and found virtually no change in σ_{PSII}. Assuming that DCMU binds randomly to Q_a, these results suggest that the deviation of the flash intensity saturation curve from a true cumulative one-hit Poisson distribution is more likely due to uneven light absorption in the highly pigmented cells than to increased RCII density per unit area of thylakoid membrane.

The maximum quantum efficiency of photosynthesis (ϕ_m, O_2 quanta^{-1}) can be calculated from the ratio of the functional to optical absorption cross-sections (11, 16, 24),

$$\phi_m = \sigma_{PSII}/(\sigma_{Chl}\ PSU_{O2}) \quad (7)$$

where PSU_{O2} is the O_2 flash yield (mol Chl/mol O_2, i.e. the so-called Emerson and Arnold number). O_2 flash yields are approximately two times higher in Fe-limited than in Fe-replete *P. tricornutum* (16). Assuming an average of 1000 Chl O_2^{-1} in Fe-replete cells and 2000 Chl O_2^{-1} in Fe-limited cells, we calculate an average ϕ_m of 0.055 in Fe-replete and 0.027 in Fe-limited cells. Note that PSU_{O2} reflects only those reaction centers capable of evolving O_2 (i.e. functional RCIIs). Assuming that each O_2 produced required four light-driven one-electron oxidation steps, and knowing the cellular Chl concentration, the number of functional RCIIs can be determined. Previous studies with Fe-limited *P. tricornutum* indicated that the number of functional RCIIs per cell was about seven times lower than in Fe-replete cells (16). In addition, Greene et al. (16) demonstrated that ϕ_m calculated from Equation 7, was identical to that calculated from photosynthesis versus irradiance (PI) parameters:

$$\phi_m = \alpha^B/a^* \quad (8)$$

where α^B is the initial slope of the PI curve. Overall, these results indicate that Fe limitation increases absorption cross-sections, but decreases the quantum efficiency and the number of functional RCIIs.

CONCLUSIONS

The results of this study indicate that Fe limitation has multiple effects on photosynthetic energy conversion in eucaryotic algae. Although Fe limitation reduces the quantum efficiency of photosynthesis, the time course of recovery from Fe limitation reveals that the reduction in efficiency is due to: (a) sluggish electron transport between Q_a and PQ; (b) a

reduction in PSII photochemical energy conversion efficiency; and (c) a reduction in energy transfer efficiency between light-harvesting Chl proteins and PSII reaction centers. The recovery process is characterized by a rapid increase in intersystem electron transport rates correlated with the synthesis of Cyt *f* and subunit IV of the Cyt b_6/f complex, a slower increase in photochemical energy conversion efficiency correlated with the synthesis of D1 and Cyt b_{559}, and a much slower accumulation of pigment protein complexes correlated with increased energy transfer to the reaction centers. The recovery process requires de novo protein synthesis.

Results of the present study provide a basis for evaluating the question of Fe limitation in the ocean. Using pump-and-probe fluorometry in the high-nutrient, low-Chl region of the eastern equatorial Pacific, we have found that natural phytoplankton populations have reduced quantum efficiencies (R.M. Greene, Z. Kolber, unpublished). Quantum efficiencies can be increased 2- to 3-fold upon addition of nanomolar concentrations of Fe, and follow similar patterns of recovery to the laboratory results presented here.

ACKNOWLEDGMENTS

We thank Dr. Joseph Hirschberg for the generous gift of the D1 antibody, and Dr. Richard Malkin for the Cyt *f* and subunit IV antibodies. We thank Steven Long, Julie LaRoche, Kevin Wyman, and Miguel Olaizola for valuable comments and discussions.

LITERATURE CITED

1. **Banse K** (1990) Does iron really limit phytoplankton production in the offshore subarctic Pacific? Limnol Oceanogr **35:** 772–775
2. **Berner T, Dubinsky Z, Wyman K, Falkowski PG** (1989) Photoadaptation and the "package" effect in *Dunaliella tertiolecta* (Chlorophyceae). J Phycol **25:** 70–78
3. **Bruce BD, Malkin R** (1991) Biosynthesis of the chloroplast cytochrome b_6f complex: studies in a photosynthetic mutant of *Lemna*. Plant Cell **3:** 203–212
4. **Cleland RE, Melis A, Neale PJ** (1986) Mechanism of photoinhibition: photochemical reaction center inactivation in system II of chloroplasts. Photosynth Res **9:** 79–88
5. **Cleveland JS, Perry MJ, Kiefer DA, Talbot MC** (1989) Maximum quantum yield of photosynthesis in the northwestern Sargasso Sea. J Mar Res **47:** 869–886
6. **Davies BH** (1976) Carotenoids. *In* TW Goodwin, ed, Chemistry and Biochemistry of Plant Pigments. Academic Press, London, pp 38–166
7. **Debus RJ, Feher G, Okamura MY** (1986) Iron-depleted reaction centers from *Rhodopseudomonas sphaeroides* R-26. Characterization and reconstitution with Fe^{2+}, Mn^{2+}, Co^{2+}, Ni^{2+}, Cu^{2+}, and Zn^{2+}. Biochemistry **25:** 2276–2287
8. **Diner BA, Petrouleas V** (1987) Q_{400}, the non-heme iron of the photosystem II iron-quinone complex. A spectroscopic probe of quinone and inhibitor binding to the reaction center. Biochim Biophys Acta **895:** 107–125
9. **Donaghay PL, Liss PS, Duce RA, Kester DR, Hanson AK, Villareal T, Tindale N, Gifford DJ** (1991) The role of episodic atmospheric nutrient inputs in the chemical and biological dynamics of oceanic ecosystems. Oceanography **4:** 62–70
10. **Doyle MP, Li L-B, Yu L, Yu C-A** (1989) Identification of a M_r = 17,000 protein as the plastoquinone-binding protein in the cytochrome b_6 complex from spinach chloroplasts. J Biol Chem **264:** 1387–1392
11. **Dubinsky Z, Falkowski PG, Wyman K** (1986) Light harvesting and utilization by phytoplankton. Plant Cell Physiol **27:** 1335–1349
12. **Dugdale RC** (1967) Nutrient limitation in the sea: dynamics, identification, and significance. Limnol Oceanogr **12:** 685–695
13. **Falkowski PG, Sukenik A, Herzig R** (1989) Nitrogen limitation in *Isochrysis galbana* (Haptophyceae). II. Relative abundance of chloroplast proteins. J Phycol **25:** 471–478
14. **Falkowski PG, Wyman K, Ley AC, Mauzerall DC** (1986) Relationship of steady-state photosynthesis to fluorescence in eucaryotic algae. Biochim Biophys Acta **849:** 183–192
15. **Falkowski PG, Ziemann D, Kolber Z, Bienfang PK** (1991) Role of eddy pumping in enhancing primary production in the ocean. Nature **352:** 55–58
16. **Greene RM, Geider RJ, Falkowski PG** (1991) Effect of iron limitation on photosynthesis in a marine diatom. Limnol Oceanogr **36:** 1772–1782
17. **Guillard RRL, Ryther JH** (1962) Studies on marine planktonic diatoms. I. *Cyclotella nana* Hustedt and *Detonula confervacae* (Cleve) Gran. Can J Microbiol **8:** 229–239
18. **Jeffrey SW, Humphrey GF** (1975) New spectrophotometric equations for determining chlorophylls a, b, c1 and c2 in higher plants, algae and natural phytoplankton. Biochem Physiol Pflanzen **167:** 191–194
19. **Kirmaier C, Holten D, Debus RJ, Feher G, Okamura MY** (1986) Primary photochemistry of iron-depleted and zinc-reconstituted reaction centers from *Rhodopseudomonas sphaeroides*. Proc Natl Acad Sci USA **83:** 6407–6411
20. **Kitajima M, Butler WL** (1975) Quenching of chlorophyll fluorescence and primary photochemistry in chloroplasts by dibromothymoquinone. Biochim Biophys Acta **376:** 105–115
21. **Kolber Z, Wyman K, Falkowski PG** (1990) Natural variability in photosynthetic energy conversion efficiency: a field study in the Gulf of Maine. Limnol Oceanogr **35:** 72–79
22. **Kolber Z, Zehr J, Falkowski PG** (1988) Effects of growth irradiance and nitrogen limitation on photosynthetic energy conversion in photosystem II. Plant Physiol **88:** 923–929
23. **Krause GH, Weis E** (1991) Chlorophyll fluorescence and photosynthesis: the basics. Annu Rev Plant Physiol Plant Mol Biol **42:** 313–349
24. **Ley AC, Mauzerall DC** (1982) Absolute absorption cross-sections for photosystem II and the minimum quantum requirement for photosynthesis in *Chlorella vulgaris*. Biochim Biophys Acta **680:** 95–106
25. **Ley AC, Mauzerall DC** (1986) The extent of energy transfer among photosystem II reaction centers. Biochim Biophys Acta **850:** 234–248
26. **Martin JH** (1991) Iron as a limiting factor in oceanic productivity. *In* PG Falkowski, AD Woodhead, eds, Primary Productivity and Biogeochemicals in the Sea. Plenum Press, New York, pp 123–137
27. **Morales F, Abadia A, Abadia J** (1991) Chlorophyll fluorescence and photon yield of oxygen evolution in iron-deficient sugar beet (*Beta vulgaris* L.) leaves. Plant Physiol **97:** 886–893
28. **Ohad I, Kyle DJ, Arntzen CJ** (1984) Membrane protein damage and repair: Removal and replacement of inactivated 32-kilodalton polypeptides in chloroplast membranes. J Cell Biol **99:** 481–485
29. **Paillotin G** (1976) Movement of excitations in the photosynthetic domain of photosystem II. J Theor Biol **58:** 237–252
30. **Terry N, Abadia J** (1986) Function of iron in chloroplasts. J Plant Nutr **9:** 609–646